

A Study of the Orbital Periods of Deeply Eclipsing SW Sextantis Stars

David Boyd¹

Abstract

Results are presented of a five-year project to study the orbital periods of eighteen deeply eclipsing novalike cataclysmic variables, collectively known as SW Sextantis stars, by combining new measurements of eclipse times with published measurements stretching back in some cases over fifty years. While the behaviour of many of these binary systems is consistent with a constant orbital period, it is evident that in several cases this is not true. Although the time span of these observations is relatively short, evidence is emerging that the orbital periods of some of these stars show cyclical variation with periods in the range 10–40 years. The two stars with the longest orbital periods, V363 Aur and BT Mon, also show secular period reduction with rates of -6.6×10^{-8} days/year and -3.3×10^{-8} days/year. New ephemerides are provided for all eighteen stars to facilitate observation of future eclipses.

1. SW Sex stars

SW Sex stars are an unofficial sub-class of cataclysmic variables (CVs), not in the General Catalogue of Variable Stars (GCVS; Samus et al. 2012), which was first proposed by Thorstensen et al. (1991) with the comment “...these objects show *mysterious* behaviour which is however highly *consistent* and *reproducible*.” They are classified in the GCVS as novalike variables. The four prototype SW Sex stars were PX And, DW UMa, SW Sex, and V1315 Aql, which all appeared to share a common set of unusual properties (see below). Since then this class has expanded to include around fifty members of which about half are definite members and the others either probable or possible based on their observed characteristics. Don Hoard maintains an on-line list of SW Sex stars (Hoard et al. 2003).

These SW Sex stars have bright accretion disks, in some cases showing occasional VY Scl-type low states, but do not have the quasi-periodic outbursts seen in dwarf novae. They are often eclipsing systems with periods mostly in the range 3–4 hours. They may exhibit either positive or negative superhumps or both. Spectroscopically they show single-peaked Balmer and HeI emission lines, not double peaked lines as expected in high inclination CVs. Superimposed on the emission lines is a transient narrow absorption feature around phase 0.5. Phase offsets are observed between the radial velocity and eclipse ephemerides. Some systems exhibit modulated circular polarization indicating magnetic accretion onto the white dwarf. There is much variation in detail between individual systems and current models of SW Sex stars have difficulty explaining all of their observed properties. The general consensus seems to be that SW Sex stars contain accretion discs which are maintained in a bright state by a high, sustained mass-transfer rate and that these discs are complex in structure and may be variously eccentric, precessing, warped, tilted, or flared at the edge. The inner edge of the disc may also be truncated if the white dwarf is magnetic. For more information, see for example Hellier (1999), Gänsicke (2005), Rodriguez-Gil (2005), Rodriguez-Gil et al. (2007a), and Rodriguez-Gil et al. (2007b). Recently it has been claimed that the majority of novalike variables in the 3–4 hour orbital period range exhibit SW Sex-like properties to some extent (see Schmidtobreick et al. 2011). If true, this suggests that the SW Sex phenomenon may be a normal stage of CV evolution.

¹ 5 Silver Lane, West Challow, Wantage, OX12 9TX, UK; davidboyd@orion.me.uk

However, the bottom line at the moment seems to be that we really don't have a full understanding of the mechanisms which operate in SW Sex stars, and how they relate to other CVs with similar periods. But, as they appear to constitute the majority of CVs with orbital periods in the range 3–4 hours, they are important and need further study.

2. Aims of the project

This project was suggested to me in early 2007 by Boris Gänsicke at Warwick University who was interested to find out if studying eclipses of SW Sex stars would reveal evidence of changes in their orbital periods. Several of these stars had not been observed systematically for many years and were in need of new observations. The idea was therefore to combine published data on eclipse times going back in some cases over fifty years with new eclipse measurements to investigate the stability of their orbital periods.

The aims of the project were, for each star:

- to research all previously published eclipse times;
- to measure new eclipse times;
- to look for evidence of a change in orbital period;
- if found, to investigate its nature;
- to update ephemerides to aid future observations.

The eighteen SW Sex stars in Hoard's list which are deeply eclipsing, observable from the UK, and bright enough to yield accurate eclipse times with amateur-sized telescopes are the subject of this project. They are listed in Table 1 in order of increasing orbital period (P_{orb}) along with the numbers of eclipse times found in the literature and new measurements reported here.

3. Previously published eclipse times

Eclipse times of minimum of these stars were discovered in over twenty different publications. For each star a list of published eclipse times obtained photographically (PG), photoelectrically (PE), or using CCD cameras was assembled along with corresponding cycle (orbit) numbers. As far as possible all times were confirmed to be in Heliocentric Julian Date (HJD). A very small number of visual eclipse times were also found but after careful consideration it was decided not to use these in this analysis because of their significantly larger and generally unknown uncertainties. In total 740 published eclipse times were located for these eighteen stars. Limitation on space prevents listing previously published eclipse times here. These are available through the AAVSO ftp site at <ftp://ftp.aavso.org/public/datasets/jboydd401.txt>.

Many published eclipse times did not specify errors. By examining the scatter in eclipse times obtained photographically their error was estimated to be, on average, 0.005d and this value was assigned to all photographic times. For photoelectric and CCD measurements published without errors each published set of data was considered separately and the root-mean-square (rms) residual of all the times in that set calculated with respect to a locally fitted linear ephemeris. This value was then assigned as an error to all the times in that set. These errors were typically in the range 0.0004d to 0.001d. In cases where the errors quoted appeared to be unrealistically small, more realistic errors were estimated by the same method. Each published time of minimum was given a weight equal to the inverse square of its error.

4. New measurements of eclipse times

Eclipses were observed using either a 0.25-m or 0.35-m telescope, both equipped with Starlight Xpress SXV-H9 CCD cameras, located at West Challow Observatory near Oxford, UK. Image scales were 1.45 and 1.21 arcsec/pixel respectively. All measurements were made unfiltered for maximum photon statistics. Images were dark subtracted and flat fielded and a magnitude for the variable in each image derived with respect to between three and five nearby comparison stars using differential aperture photometry.

The dominant light source in these systems is the bright accretion disk, and its progressive eclipse by the secondary star results in eclipse profiles which are generally V-shaped with a rounded minimum. A quadratic fit was applied to the lower part of each eclipse from which the eclipse time of minimum and an associated analytical error were obtained. The magnitude at minimum was also obtained from this fit, enabling eclipse depths to be estimated. Some of these stars exhibit relatively large random fluctuations in light output which can persist during eclipses, indicating the source of these fluctuations has not been eclipsed. This can result in significant distortion of their eclipse profiles and consequently larger scatter in their measured times of minimum. In general it was found that the analytical errors from the quadratic fits underestimated the real scatter in eclipse times. By examining this scatter for each star over a short interval during which the eclipse times were varying linearly, a multiplying factor was found which was then applied to the analytical errors. For stars with the smoothest eclipses, a factor of 3 gave errors consistent with the scatter of eclipse times while for the most distorted eclipses a factor of 7 was required. Each measured time of minimum was given a weight equal to the inverse square of its associated error. All new times of minimum were converted to HJD. As shown in Table 1, 298 new eclipse times were measured, increasing the number of available eclipse times for these stars by 40%.

Initially a constant orbital period for each star was assumed and a linear ephemeris computed based only on published eclipse times. Predictions were then made of the expected times of future eclipses. Although in some cases these predictions were found to be inaccurate by up to an hour, in all cases it was possible to project the historical cycle count forward and unambiguously assign cycle numbers to new eclipses as they were observed.

For each star we now had the HJD of the time of minimum for every measured eclipse plus an error and a corresponding cycle number. New eclipse times measured for the eighteen stars in the project are listed in Table 2.

5. O–C analysis

For each star a constant orbital period was assumed and a weighted linear ephemeris was calculated based on all available eclipse times, both published and new. O–C (Observed minus Calculated) values for the time of each eclipse with respect to this linear ephemeris were calculated and an O–C diagram generated for each star. O–C values following the horizontal line at $O-C = 0$ would confirm that the orbital period was indeed constant. O–C values following an upwards curve would indicate that the period was increasing while a downwards curve would indicate that the period was decreasing. Sinusoidal behaviour would indicate that the orbital period was varying in a cyclical way, alternately increasing and decreasing.

6. Eclipsing SW Sex stars with orbital periods less than 4 hours

Most of the thirteen eclipsing SW Sex stars with orbital periods less than 4 hours have O–C diagrams which appear to be consistent with having a constant orbital period over the time span covered by the available observations, in some cases more than thirty years. However, in a few cases there is an indication of possible non-linear behaviour. This was investigated by applying a weighted sine fit to their O–C values using Period04 (Lenz and Breger 2005) and comparing the rms residuals of linear and sinusoidal ephemerides. The conclusion was that ten of the thirteen stars were consistent with having linear ephemerides and therefore a constant orbital period while three, SW Sex, LX Ser, and UU Aqr, gave at least 20% smaller rms residuals for sinusoidal ephemerides indicating possible cyclical variation of their orbital periods.

Linear ephemerides for these thirteen SW Sex stars are given in Table 3. These should provide an accurate basis for predicting the times of future eclipses. Table 4 lists the parameters of possible cyclical variation and rms residuals of sinusoidal and linear ephemerides for SW Sex, LX Ser, and UU Aqr.

Figure 1 shows O–C diagrams for the ten SW Sex stars with orbital periods less than 4 hours which are consistent with linear ephemerides. Previously published observations are marked as black dots and new eclipse times as red squares in this and subsequent figures. The larger scatter for some stars is primarily due to the less regular shape of their eclipses as noted above. Figure 2 shows O–C diagrams for SW Sex, LX Ser, and UU Aqr with dashed lines representing their sinusoidal ephemerides.

Given the length of their cyclical periods relative to the observed coverage and their relatively small amplitudes, more data are required to substantiate these cyclical interpretations. We do, however, note that similar behaviour has been recorded in several other eclipsing CVs, see for example Borges et al. (2008) and references therein.

7. Eclipsing SW Sex stars with orbital periods greater than 4 hours

Five of the SW Sex stars have orbital periods longer than 4 hours: RW Tri, 1RXS J064434.5+334451, AC Cnc, V363 Aur, and BT Mon. For all these stars the eclipse times appear, to varying degrees, to be inconsistent with the assumption of a constant orbital period. Each of these stars is now considered individually.

7.1. *RW Tri*

A total of 115 published and 21 new eclipse times are available for RW Tri starting in 1957. The O–C diagram for RW Tri representing the residuals to a linear ephemeris with long-term average orbital period 0.231883193(2) day is shown in Figure 3a. The scatter in the data is sufficiently large that a time calibration problem with some of the published times must be considered a possibility. We decided to exclude the 11 eclipse times around HJD 2449600 from subsequent analysis as their O–C values were more than 5 minutes larger than those before and after. Between approximately HJD 2442000 and HJD 2450000 the period slowly decreased. It then started to increase and is currently longer than the long-term average. Taken as a whole, the data suggest cyclical variation of the orbital period. A weighted sine fit to the O–C data using Period04 gives the results listed in Table 5 and shown as a dashed line in Figure 3a. Also listed in Table 5 are the rms residuals of sinusoidal and linear fits indicating that sinusoidal interpretation is statistically favoured. However, given the large scatter in the data and the fact that just over one possible cycle has been observed, a convincing

analysis will require data over a much longer time span. An earlier analysis by Africano et al. (1978) suggested sinusoidal variation with a period of either 7.6 or 13.6 years but with the addition of more recent data neither of these periods survives.

A linear ephemeris fitted to the data over the past seven years which should be useful for predicting eclipses in the near future is given in Table 3.

The out-of-eclipse magnitude of RW Tri, including early measurements reported by Walker (1963), observations from the AAVSO International Database and from ASAS (Pojmański et al. 2005), and new observations reported here, is plotted in Figure 3b. This shows a slight brightening around HJD 2450000 but otherwise little change. Eclipse depth has remained approximately constant over the observed time span (Figure 3c). Table 6 lists measurements of eclipse depth for the five stars with long orbital periods.

7.2. 1RXS J064434.5+334451

Twenty unpublished eclipse times for 1RXS J064434.5+334451 from 2005 to 2008 were kindly provided by David Sing and Betsy Green, who first identified this star as a CV (Sing et al. 2007). The first times reported here were in 2010 and these were consistent with those of Sing and Green, giving the orbital period 0.26937447(4) day and the linear eclipse ephemeris given in Table 3.

Surprisingly, eclipses in March 2011 were about three minutes late relative to this ephemeris. This behaviour has since continued with most eclipses occurring between two and four minutes later than expected assuming a linear ephemeris based on observations up to and including 2010 (HJD < 2455500 – see Figure 4a). Since March 2011 the mean orbital period has been slightly shorter at 0.2693741(2) day. The out-of-eclipse magnitude experienced a rise prior to, and a dip following, the O–C discontinuity (Figure 4b). Eclipses became, temporarily, about 10% deeper after the O–C discontinuity (Figure 4c and Table 6).

7.3. AC Cnc

For AC Cnc, 46 published and 11 new eclipse times are available and fitting a linear ephemeris to these gives the O–C diagram shown in Figure 5a. Times measured before 1980 are photographic and have a large scatter. Using the more precise photoelectric and CCD measurements since 1980 (HJD > 2444000) gives an orbital period of 0.30047738(1) day and the linear eclipse ephemeris given in Table 3.

A recent paper by Qian et al. (2007) argues for a decreasing orbital period and also proposes a third body in the system causing sinusoidal modulation in the O–C diagram. A quadratic ephemeris calculated using the more reliable photoelectric and CCD measurements following HJD 2444000 and including the new times reported here gives a rate of period change of $2.1(2.2) \times 10^{-9}$ days/year, considerably smaller than the rate of $12.4(4.4) \times 10^{-9}$ days/year found by Qian et al. and consistent with no secular period change. However, there is an indication of cyclical behaviour in the O–C diagram in Figure 5a. A weighted sine fit to the O–C data after HJD 2444000 gives the results listed in Table 5 and shown as a dashed line in Figure 5a. This is a shorter period and smaller amplitude than proposed by Qian et al. Observations over a much longer period are required to establish the reality and true parameters of this modulation. With few measurements available, there is little indication of variation in either the out-of-eclipse magnitude of AC Cnc (Figure 5b) or the eclipse depth (Figure 5c and Table 6).

7.4. V363 Aur (also known as Lanning 10)

The data for V363 Aur comprise 18 published and 27 new eclipse times and show a significant curvature in the O–C diagram with respect to a linear ephemeris, indicating a reducing orbital period (Figure 6a). A quadratic ephemeris, shown as a dashed line in Figure 6a, gives a mean rate of period change of $dP/dt = -6.6(2) \times 10^{-8}$ days/year over the 31 years covered by the data. The O–C residuals to this quadratic ephemeris (Figure 6b) show an apparently cyclical variation. A weighted sine fit to the residuals of the quadratic ephemeris gives the results listed in Table 5 and shown as a dashed line in Figure 6b, but these results must be considered speculative as only one cycle has been observed.

Over the past six years the mean orbital period has been 0.32124073(3) day and the eclipse times are well fitted by the linear ephemeris given in Table 3.

Figure 6c shows the out-of-eclipse magnitude of V363 Aur obtained from the AAVSO database plus our new measurements. Although the scatter is large, there appears to have been a slight dip centred around HJD 2449000. Figure 6d and Table 6 show the depth of eclipses of V363 Aur over the same interval. Although there are little data in the early years, recently there has been a progressive reduction in eclipse depth.

7.5. BT Mon

BT Mon is the progenitor system of a classical nova outburst observed in 1939. There are 8 published eclipse times plus 14 new times covering a 34 year time span. An O–C diagram with respect to a linear ephemeris shows significant curvature indicating a reducing orbital period (Figure 7a). A quadratic ephemeris, shown as a dashed line in Figure 7a, gives a mean rate of period change of $dP/dt = -3.3(2) \times 10^{-8}$ days/year. The O–C residuals to this quadratic ephemeris are shown in Figure 7b along with a dashed line indicating the results of a weighted sine fit whose parameters are listed in Table 5. This sinusoidal ephemeris is marginally favoured over the quadratic ephemeris although, as before, this conclusion must remain tentative until more data are available.

Published eclipse times are scarce in the middle of this time span. Magnitude measurements of BT Mon obtained with the Roboscope system (Honeycutt 2003) between 1991 and 2005 were kindly provided by Kent Honeycutt. The Roboscope data were divided into two groups, before and after the start of 1999. By adopting mean orbital periods from the above quadratic ephemeris for each of these time intervals, two additional eclipse times have been synthesised using the Roboscope data. These have larger errors than directly measured eclipse times and are shown as green triangles in Figures 7. They were not used in the above analysis but are consistent with its results and slightly favour the sinusoidal interpretation.

Over the last seventeen years the mean orbital period has been 0.33381322(2) day and eclipse times in the near future may be represented by the linear ephemeris given in Table 3.

Plotting out-of-eclipse magnitudes from Roboscope together with our new data (Figure 7c), we see a noticeable dip around HJD 2451000 followed by a gradual increase. Although there are little data, the eclipse depth shows a slowly decreasing trend over the same interval (Figure 7d and Table 6).

8. Conclusions

When this project started, most published analyses of SW Sex stars concluded that they had constant orbital periods. While the new data confirm that this is true for many of these stars, for some it is clearly not the case. There is a significant difference between the behaviour of stars with orbital

periods below and above 4 hours. Below 4 hours, ten of the thirteen stars appear to have constant orbital periods with three showing possible signs of low amplitude cyclical variation. The longer period stars all show more dynamic behaviour with either a sudden change of orbital period or larger amplitude cyclical variation, either with or without a secular period change.

Eclipse times for all these stars will continue to be monitored to see if those with constant periods maintain this behaviour and in the other more interesting cases with longer orbital periods to discover what light further data will shed on the tentative interpretations presented here.

9. Acknowledgements

I am grateful to Boris Gänsicke for suggesting this project and for his continuing support and encouragement. I am indebted to David Sing and Betsy Green for providing unpublished data on 1RXS J064434.5+334451 and to Kent Honeycutt for providing unpublished Roboscope data on BT Mon. I acknowledge with thanks that this research has made use of variable star observations from the AAVSO International Database contributed by researchers worldwide, data from the All Sky Automated Survey, and from NASA's Astrophysics Data System. Helpful comments from an anonymous referee have improved the paper.

References

- Africano, J. L., Nather, R. E., Patterson, J., Robinson, E. L., and Warner, B. 1978, *Publ. Astron. Soc. Pacific*, 90, 568.
- Borges, B. W., Baptista, R., Papadimitriou, C., and Giannakis, O. 2008, *Astron. Astrophys.*, 480, 481.
- Gaensicke, B. 2005, in *The Astrophysics of Cataclysmic Variables and Related Objects*, ed. J. -M. Hameury and J. -P. Lasota. ASP Conf. Ser. 330, Astron. Soc. Pacific, San Francisco, 3.
- Hellier, C. 1999, *New Astron. Rev.*, 44, 131.
- Hoard, D., Szkody, P., Froning, C. S., Long, K. S., and Knigge, C. 2003, *Astron. J.*, 126, 2473 (see also <http://www.dwhoard.com/home/biglist>).
- Honeycutt, R. K. 2003, *Bull. Amer. Astron. Soc.*, 35, 752.
- Lenz, P., and Breger M. 2005, *Commun. Asteroseismology*, 146, 53.
- Pojmański, G., Pilecki, B., and Szczygiel, D. 2005, *Acta Astron.*, 55, 275.
- Qian, S. -B., Dai, Z. -B., He, J. -J., Yuan, J. Z., Xiang, F. Y., and Zejda, M. 2007, *Astron. Astrophys.*, 466, 589.
- Rodriguez-Gil, P. 2005, in *The Astrophysics of Cataclysmic Variables and Related Objects*, ed. J. -M. Hameury and J. -P. Lasota. ASP Conf. Ser. 330, Astron. Soc. Pacific, San Francisco, 335.
- Rodriguez-Gil, P., Schmidtobreick, L., and Gänsicke, B. T. 2007a, *Mon. Not. Roy. Astron. Soc.*, 374, 1359.
- Rodriguez-Gil, P., et al. 2007b, *Mon. Not. Roy. Astron. Soc.*, 377, 1747.
- Samus, N. N., et al. 2012, *General Catalogue of Variable Stars* (<http://www.sai.msu.su/gcvs/gcvs/>).
- Schmidtobreick, L., Rodriguez-Gil, P., and Gänsicke, B. T. 2011, <http://adsabs.harvard.edu/abs/2011arXiv1111.6678S>
- Sing, D. K., Green, E. M., Howell, S. B., Holberg, J. B., Lopez-Morales, M., Shaw, J. S., and Schmidt, G. D. 2007, *Astron. Astrophys.*, 474, 951.
- Thorstensen, J., Ringwald, F. A., Wade, R. A., Schmidt, G. D., and Norsworthy, J. E. 1991, *Astron. J.*, 102, 272.
- Walker, M. F. 1963, *Astrophys. J.*, 137, 485.

Table 1. Eclipsing SW Sex stars studied in this project.

Name	P _{orb} (hrs)	Previously published eclipse times	New eclipse times reported here
HS 0728+6738	3.21	14	24
SW Sex	3.24	32	11
DW UMa	3.28	176	20
HS 0129+2933 = TT Tri	3.35	27	11
V1315 Aql	3.35	71	16
PX And	3.51	38	22
HS 0455+8315	3.57	5	15
HS 0220+0603	3.58	13	13
BP Lyn	3.67	16	13
BH Lyn	3.74	29	16
LX Ser	3.80	50	10
UU Aqr	3.93	50	15
V1776 Cyg	3.95	12	17
RW Tri	5.57	115	21
1RXS J064434.5+334451	6.47	20	22
AC Cnc	7.21	46	11
V363 Aur = Lanning 10	7.71	18	27
BT Mon	8.01	8	14
Total		740	298

Table 2. Eclipse times for stars measured in this project with errors and corresponding cycle numbers.

Eclipse time of minimum (HJD)	Error (d)	Cycle number	Eclipse time of minimum (HJD)	Error (d)	Cycle number
HS 0728+6738			2454185.43702	0.00044	72965
2453810.40077	0.00041	13539	2454186.38145	0.00029	72972
2453836.45653	0.00024	13734	2454553.41407	0.00048	75692
2453851.42254	0.00023	13846	2454564.34410	0.00020	75773
2453853.42648	0.00013	13861	2454906.41325	0.00019	78308
2454174.51418	0.00022	16264	2454907.49269	0.00019	78316
2454181.32859	0.00025	16315	2455260.35696	0.00018	80931
2454185.33706	0.00025	16345	2455278.43821	0.00012	81065
2454186.40643	0.00024	16353	2455630.35814	0.00026	83673
2454473.42029	0.00023	18501	2455660.44910	0.00014	83896
2454493.33001	0.00023	18650	2455662.33853	0.00028	83910
2454507.35967	0.00039	18755	DW UMa		
2454835.39541	0.00032	21210	2454181.41978	0.00019	58214
2454891.38182	0.00010	21629	2454185.38111	0.00030	58243
2454895.39084	0.00009	21659	2454224.45051	0.00044	58529
2454907.41644	0.00022	21749	2454473.34780	0.00038	60351
2455188.41832	0.00021	23852	2454564.46466	0.00020	61018
2455191.35834	0.00014	23874	2454580.44785	0.00033	61135
2455200.31029	0.00019	23941	2454580.58433	0.00027	61136
2455515.38459	0.00024	26299	2454588.37104	0.00029	61193
2455520.32865	0.00038	26336	2454588.50711	0.00019	61194
2455533.42346	0.00028	26434	2454593.42488	0.00022	61230
2455889.38551	0.00036	29098	2454596.43092	0.00034	61252
2455891.39036	0.00024	29113	2454884.39723	0.00025	63360
2455893.39432	0.00019	29128	2454892.32009	0.00025	63418
SW Sex			2455239.30026	0.00022	65958

Eclipse time of minimum (HJD)	Error (d)	Cycle number
2455263.34322	0.00015	66134
2455270.31000	0.00014	66185
2455278.37037	0.00017	66244
2455627.39978	0.00017	68799
2455628.35604	0.00020	68806
2455629.31205	0.00030	68813
HS 0129+2933		
2454061.46332	0.00014	10892
2454081.29219	0.00016	11034
2454086.45848	0.00008	11071
2455106.37036	0.00038	18375
2455188.47729	0.00030	18963
2455191.27007	0.00019	18983
2455460.49099	0.00013	20911
2455533.38206	0.00022	21433
2455827.45860	0.00014	23539
2455835.41776	0.00016	23596
2455836.39518	0.00010	23603
V1315 Aql		
2454272.50437	0.00018	59916
2454306.44865	0.00027	60159
2454313.43262	0.00072	60209
2454651.48330	0.00048	62629
2454670.48100	0.00046	62765
2454810.31097	0.00082	63766
2455004.47952	0.00029	65156
2455006.43480	0.00049	65170
2455038.42351	0.00055	65399
2455052.39293	0.00070	65499
2455463.36184	0.00047	68441
2455464.33978	0.00036	68448
2455490.32143	0.00026	68634
2455777.38468	0.00040	70689
2455783.39087	0.00040	70732
2455903.24546	0.00047	71590
PX And		
2454318.44729	0.00051	34708
2454319.47234	0.00046	34715
2454325.47261	0.00036	34756
2454448.40773	0.00061	35596
2454473.28943	0.00051	35766
2454503.29163	0.00022	35971
2454761.45718	0.00049	37735
2454770.38547	0.00069	37796
2455064.40680	0.00108	39805
2455066.45577	0.00069	39819
2455173.29503	0.00032	40549
2455186.32065	0.00020	40638
2455188.36884	0.00125	40652
2455191.29553	0.00055	40672
2455201.24653	0.00014	40740
2455460.43876	0.00028	42511
2455495.26963	0.00061	42749
2455515.46733	0.00025	42887
2455795.43984	0.00024	44800
2455819.44115	0.00069	44964
2455823.39248	0.00044	44991
2455901.25250	0.00064	45523

Eclipse time of minimum (HJD)	Error (d)	Cycle number
HS 0455+8315		
2454061.40139	0.00016	14807
2454063.48351	0.00020	14821
2454078.35643	0.00014	14921
2454112.41335	0.00017	15150
2454114.49593	0.00023	15164
2454115.38831	0.00017	15170
2454895.44552	0.00018	20415
2454906.45070	0.00013	20489
2454907.34318	0.00026	20495
2455065.43666	0.00029	21558
2455495.39753	0.00032	24449
2455519.49112	0.00017	24611
2455526.48082	0.00018	24658
2455835.38030	0.00021	26735
2455850.40114	0.00018	26836
HS 0220+0603		
2454061.32109	0.00048	10038
2454081.31479	0.00032	10172
2454081.46403	0.00018	10173
2454086.38783	0.00026	10206
2455156.35608	0.00028	17377
2455188.43603	0.00027	17592
2455200.37262	0.00034	17672
2455490.43180	0.00028	19616
2455495.35697	0.00031	19649
2455515.34977	0.00031	19783
2455533.40410	0.00029	19904
2455867.48013	0.00024	22143
2455884.48964	0.00012	22257
BP Lyn		
2454186.44462	0.00069	41257
2454891.36892	0.00095	45870
2454906.49781	0.00084	45969
2455239.32473	0.00058	48147
2455260.41122	0.00042	48285
2455263.31415	0.00049	48304
2455571.38461	0.00074	50320
2455594.30701	0.00042	50470
2455619.52087	0.00059	50635
2455914.44759	0.00041	52565
2455930.34125	0.00063	52669
2455932.32762	0.00066	52682
2455942.41314	0.00039	52748
BH Lyn		
2454181.48914	0.00029	44915
2454186.32132	0.00042	44946
2454199.41436	0.00053	45030
2454482.32954	0.00048	46845
2454834.45234	0.00046	49104
2454884.33284	0.00052	49424
2455247.36666	0.00027	51753
2455260.46000	0.00033	51837
2455267.31793	0.00059	51881
2455594.34608	0.00035	53979
2455628.32676	0.00041	54197
2455670.41251	0.00040	54467
2455675.40111	0.00031	54499

Eclipse time of minimum (HJD)	Error (d)	Cycle number
2455895.34197	0.00038	55910
2455902.35570	0.00039	55955
2455941.32605	0.00040	56205
LX Ser		
2454316.41420	0.00032	63266
2454628.52570	0.00023	65236
2454976.44297	0.00038	67432
2454994.50414	0.00026	67546
2455001.47525	0.00033	67590
2455037.43960	0.00020	67817
2455662.45627	0.00040	71762
2455663.40637	0.00045	71768
2455672.43730	0.00041	71825
2455778.42860	0.00031	72494
UU Aqr		
2454323.44995	0.00046	48760
2454357.47405	0.00027	48968
2454365.48955	0.00036	49017
2454728.47437	0.00051	51236
2454735.34486	0.00034	51278
2454736.32601	0.00056	51284
2454789.32574	0.00032	51608
2455038.45994	0.00069	53131
2455059.39716	0.00052	53259
2455106.34585	0.00043	53546
2455469.49424	0.00052	55766
2455490.26865	0.00048	55893
2455778.49715	0.00019	57655
2455795.50952	0.00019	57759
2455893.33048	0.00019	58357
V1776 Cyg		
2454238.48406	0.00059	45659
2454254.46252	0.00044	45756
2454306.51977	0.00050	46072
2454314.42730	0.00053	46120
2454646.54029	0.00092	48136
2454668.44971	0.00092	48269
2454670.42804	0.00080	48281
2454770.42363	0.00115	48888
2454994.46940	0.00068	50248
2455037.46488	0.00052	50509
2455057.39969	0.00051	50630
2455176.34096	0.00062	51352
2455460.34923	0.00100	53076
2455494.45030	0.00101	53283
2455778.46040	0.00052	55007
2455849.46194	0.00052	55438
2455893.28160	0.00088	55704
RW Tri		
2454392.38737	0.00024	57197
2454419.51756	0.00027	57314
2454447.34346	0.00020	57434
2454789.37226	0.00041	58909
2454810.47333	0.00064	59000
2454835.28542	0.00050	59107
2455063.45767	0.00047	60091
2455106.35664	0.00047	60276
2455172.44338	0.00026	60561

Eclipse time of minimum (HJD)	Error (d)	Cycle number
2455487.34152	0.00042	61919
2455490.35562	0.00017	61932
2455533.48590	0.00023	62118
2455822.41233	0.00026	63364
2455828.44141	0.00023	63390
2455867.39741	0.00048	63558
2455881.31079	0.00014	63618
2455889.42621	0.00028	63653
2455914.23796	0.00028	63760
2455950.41154	0.00024	63916
2455953.42610	0.00051	63929
2455957.36910	0.00018	63946
IRXS J064434.5+334451		
2455307.42924	0.00074	7067
2455310.39210	0.00056	7078
2455313.35557	0.00049	7089
2455627.44814	0.00048	8255
2455629.33392	0.00043	8262
2455634.45149	0.00035	8281
2455655.46296	0.00045	8359
2455658.42635	0.00025	8370
2455682.39947	0.00042	8459
2455685.36351	0.00051	8470
2455850.48993	0.00045	9083
2455854.53082	0.00023	9098
2455891.43482	0.00015	9235
2455905.44214	0.00063	9287
2455914.33106	0.00043	9320
2455924.29847	0.00046	9357
2455932.37955	0.00032	9387
2455949.35041	0.00027	9450
2455953.38926	0.00037	9465
2455957.43085	0.00052	9480
2455959.31737	0.00024	9487
2455960.39430	0.00028	9491
AC Cnc		
2454199.45197	0.00026	32978
2454507.44198	0.00021	34003
2454891.45161	0.00036	35281
2454892.35306	0.00032	35284
2455260.43835	0.00023	36509
2455270.35440	0.00042	36542
2455619.50814	0.00082	37704
2455630.32565	0.00024	37740
2455675.39674	0.00047	37890
2455949.43118	0.00029	38802
2455959.34723	0.00034	38835
V363 Aur		
2454181.39163	0.00043	29957
2454392.44674	0.00017	30614
2454447.37885	0.00024	30785
2454471.47221	0.00031	30860
2454473.39980	0.00037	30866
2454810.38137	0.00031	31915
2454827.40653	0.00042	31968
2454835.43772	0.00044	31993
2454891.33360	0.00054	32167
2454892.29747	0.00021	32170

Eclipse time of minimum (HJD)	Error (d)	Cycle number
2455188.48144	0.00054	33092
2455191.37255	0.00040	33101
2455200.36736	0.00026	33129
2455515.50429	0.00013	34110
2455516.46885	0.00021	34113
2455524.49896	0.00034	34138
2455526.42586	0.00026	34144
2455627.29626	0.00020	34458
2455634.36298	0.00020	34480
2455649.46157	0.00047	34527
2455854.41351	0.00026	35165
2455888.46463	0.00016	35271
2455891.35618	0.00021	35280
2455905.49122	0.00039	35324
2455914.48560	0.00015	35352
2455950.46438	0.00013	35464

Eclipse time of minimum (HJD)	Error (d)	Cycle number
2455954.31900	0.00028	35476
BT Mon		
2454447.47617	0.00043	32820
2454891.44778	0.00052	34150
2454892.44988	0.00045	34153
2455238.27878	0.00050	35189
2455239.28089	0.00082	35192
2455257.30609	0.00035	35246
2455260.31093	0.00041	35255
2455277.33531	0.00068	35306
2455571.42510	0.00058	36187
2455595.46030	0.00062	36259
2455600.46698	0.00093	36274
2455619.49354	0.00048	36331
2455960.31808	0.00089	37352
2455968.33013	0.00047	37376

Table 3. Linear ephemerides for the SW Sex stars in the project. For RW Tri, 1RXS J064434.5+334451, AC Cnc, V363 Aur, and BT Mon this linear ephemeris only represents behaviour in the recent past. Over longer time intervals their behaviour is more complex (see text).

HS 0728+6738	$2452001.32739(8) + 0.133619437(4) * E$
SW Sex	$2444339.64968(11) + 0.134938490(2) * E$
DW UMa	$2446229.00601(8) + 0.136606547(2) * E$
HS 0129+2933 = TT Tri	$2452540.53218(9) + 0.139637462(6) * E$
V1315 Aql	$2445902.84037(10) + 0.139689961(2) * E$
PX And	$2449238.83661(17) + 0.146352746(4) * E$
HS 0455+8315	$2451859.24679(15) + 0.148723901(8) * E$
HS 0220+0603	$2452563.57407(7) + 0.149207696(5) * E$
BP Lyn	$2447881.85799(23) + 0.152812531(6) * E$
BH Lyn	$2447180.33522(41) + 0.155875629(8) * E$
LX Ser	$2444293.02345(18) + 0.158432492(3) * E$
UU Aqr	$2446347.26651(6) + 0.163580450(2) * E$
V1776 Cyg	$2446716.67956(27) + 0.164738679(6) * E$
RW Tri	$2441129.35318(49) + 0.231883392(9) * E$
1RXS J064434.5+334451	$2453403.75955(12) + 0.26937447(4) * E$
AC Cnc	$2444290.30892(36) + 0.30047738(1) * E$
V363 Aur = Lanning 10	$2444557.98318(89) + 0.32124073(3) * E$
BT Mon	$2443491.72616(45) + 0.33381322(2) * E$

Table 4. Parameters of possible cyclical variation in orbital period for SW Sex, LX Ser, and UU Aqr.

	Cyclical period (year)	Semi-amplitude (sec)	Sinusoidal ephemeris rms residual	Linear ephemeris rms residual
SW Sex	24.0(7)	69(5)	32.1	65.2
LX Ser	28(2)	48(6)	55.7	69.4
UU Aqr	20.3(6)	48(4)	34.9	43.6

Table 5. Parameters of possible cyclical variation in orbital period for RW Tri, AC Cnc, V363 Aur, and BT Mon (* only including data after HJD 2444000).

	Cyclical period (year)	Semi-amplitude (sec)	Sinusoidal ephemeris rms residual	Linear ephemeris rms residual	Quadratic ephemeris rms residual
RW Tri	36.7(4)	161(5)	80.8	128.0	
AC Cnc*	13.5(3)	140(13)	106.8	141.3	139.5
V363 Aur	27.7(7)	119(6)	58.8		92.2
BT Mon	29(2)	113(15)	62.0		67.7

Table 6. Eclipse depth measured in this project for RW Tri, 1RXS J064434.5+334451, AC Cnc, V363 Aur, and BT Mon.

Eclipse time (HJD)	Eclipse depth (mag)	Eclipse time (HJD)	Eclipse depth (mag)
RW Tri		AC Cnc	
2454392.38737	1.72	2454199.45197	0.96
2454419.51756	1.84	2454507.44198	1.04
2454447.34346	1.96	2454891.45161	0.94
2454810.47333	1.84	2454892.35306	0.92
2454835.28542	1.63	2455260.43835	1.00
2455063.45767	1.76	2455630.32565	0.87
2455106.35664	1.92	2455949.43118	1.14
2455172.44338	1.89	V363 Aur	
2455487.34152	1.78	2454392.44674	0.80
2455490.35562	1.71	2454447.37885	0.71
2455533.48590	1.84	2454471.47221	0.90
2455822.41233	1.62	2454473.39980	0.83
2455828.44141	1.43	2454810.38137	0.62
2455867.39741	1.59	2454827.40653	0.66
2455881.31079	1.81	2454835.43772	0.77
2455889.42621	1.89	2454892.29747	0.64
2455914.23796	1.69	2455191.37255	0.76
2455950.41154	2.06	2455515.50429	0.56
2455953.42610	1.97	2455516.46885	0.68
2455957.36910	1.56	2455524.49896	0.60
1RXS J064434.5+334451		2455526.42586	0.48
2455307.42924	1.13	2455627.29626	0.62
2455310.39210	1.06	2455634.36298	0.68
2455627.44814	1.26	2455649.46157	0.69
2455629.33392	1.27	2455854.41351	0.58
2455634.45149	0.90	2455888.46463	0.53
2455655.46296	1.22	2455891.35618	0.62
2455658.42635	1.29	2455905.49122	0.65
2455682.39947	1.31	2455950.46438	0.71
2455685.36351	1.23	BT Mon	
2455850.48993	1.17	2454891.44778	1.74
2455854.53082	1.11	2454892.44988	1.82
2455891.43482	1.12	2455257.30609	2.01
2455905.44214	1.13	2455260.31093	1.90
2455914.33106	1.08	2455277.33531	1.96
2455932.37955	1.14	2455571.42510	1.61
2455949.35041	1.02	2455960.31808	1.49
2455953.38926	1.07	2455968.33013	1.62
2455957.43085	0.94		
2455959.31737	0.97		
2455960.39430	1.14		

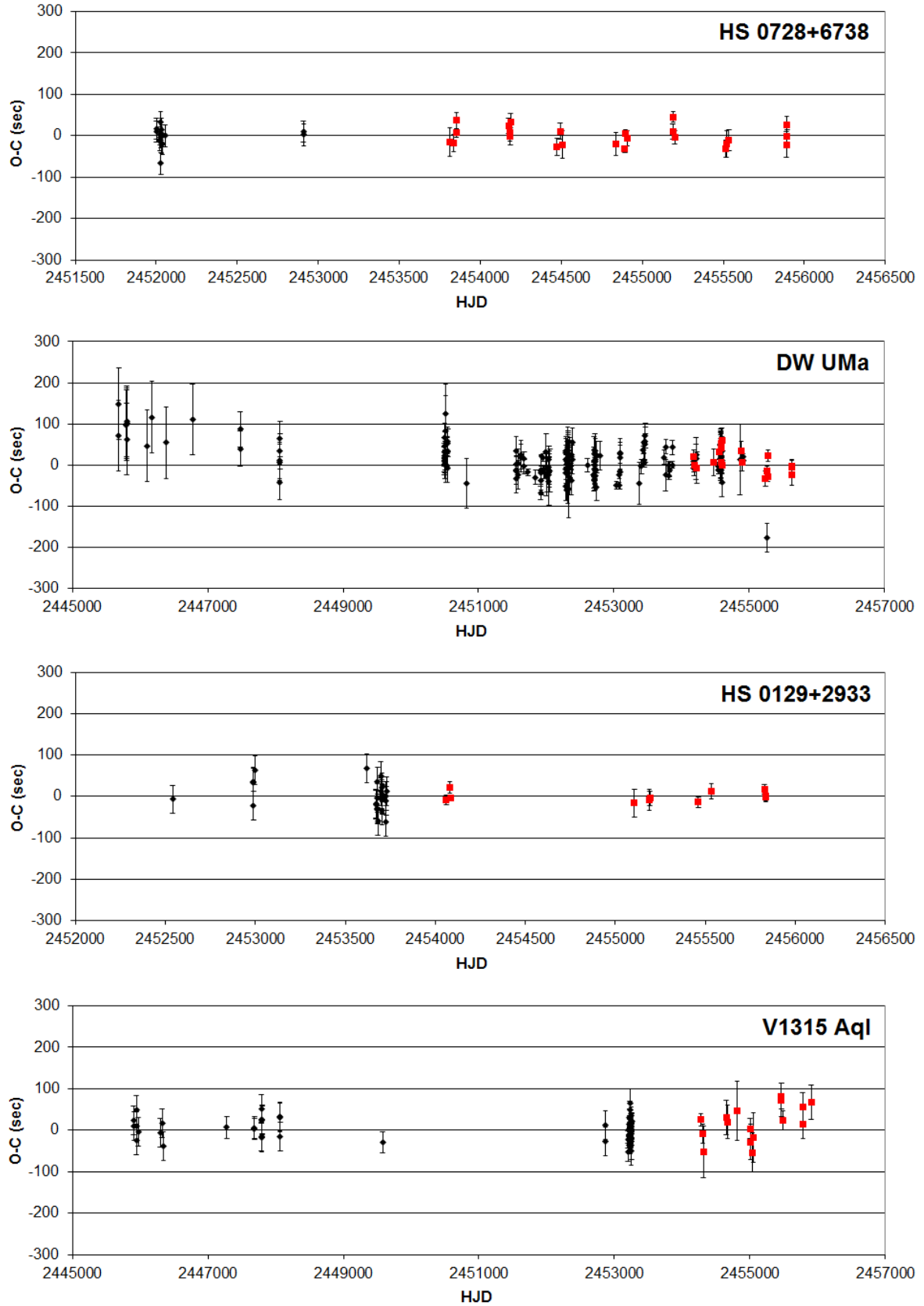


Figure 1. O–C diagrams with respect to the linear ephemerides in Table 3 for those SW Sex stars with $P_{orb} < 4$ hours which are consistent with constant orbital periods. Previously published observations are marked as black dots and new eclipse times as red squares in this and subsequent figures (continued on next page).

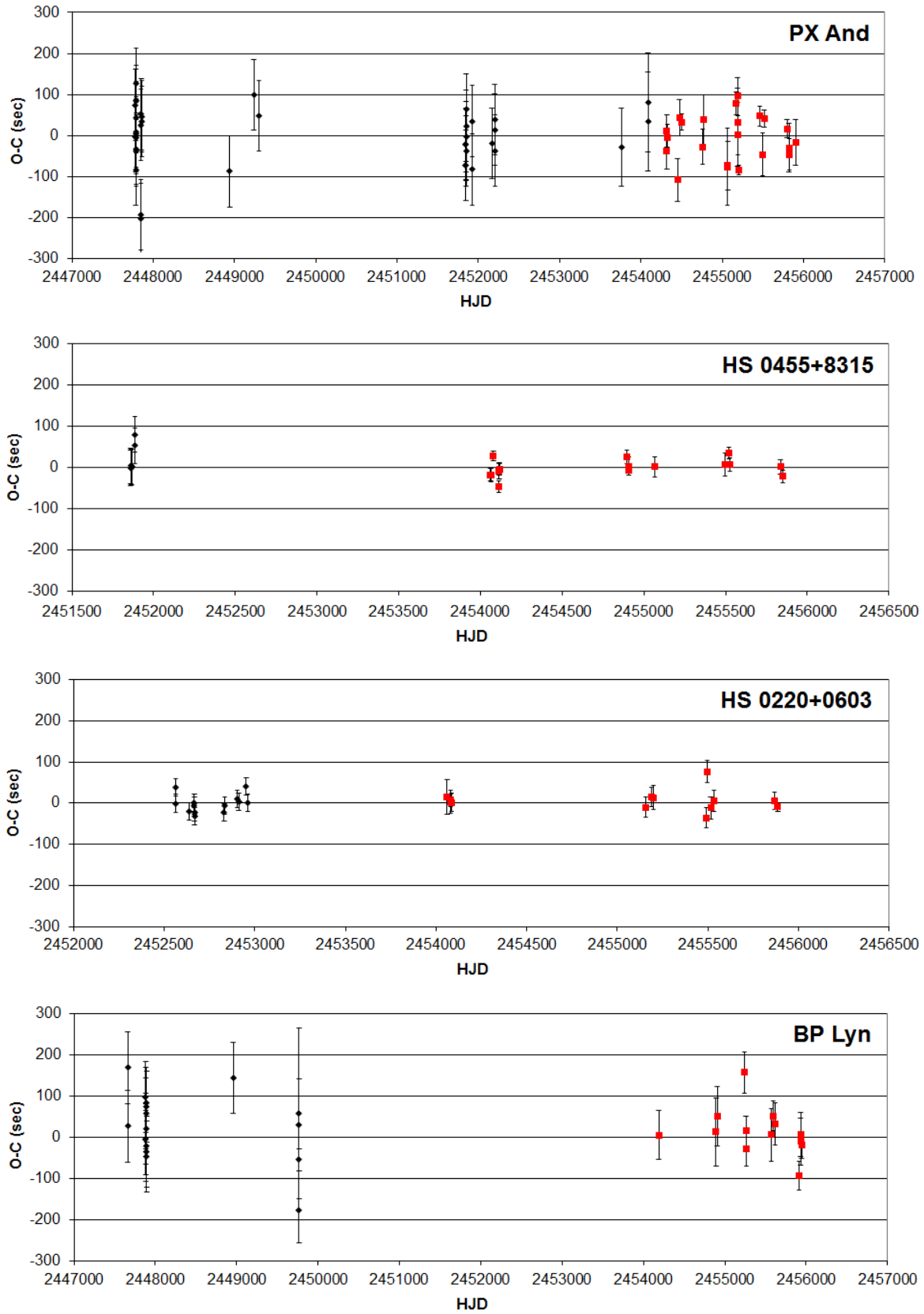


Figure 1. O-C diagrams with respect to the linear ephemerides in Table 3 for those SW Sex stars with $P_{orb} < 4$ hours which are consistent with constant orbital periods. Previously published observations are marked as black dots and new eclipse times as red squares in this and subsequent figures (continued on next page).

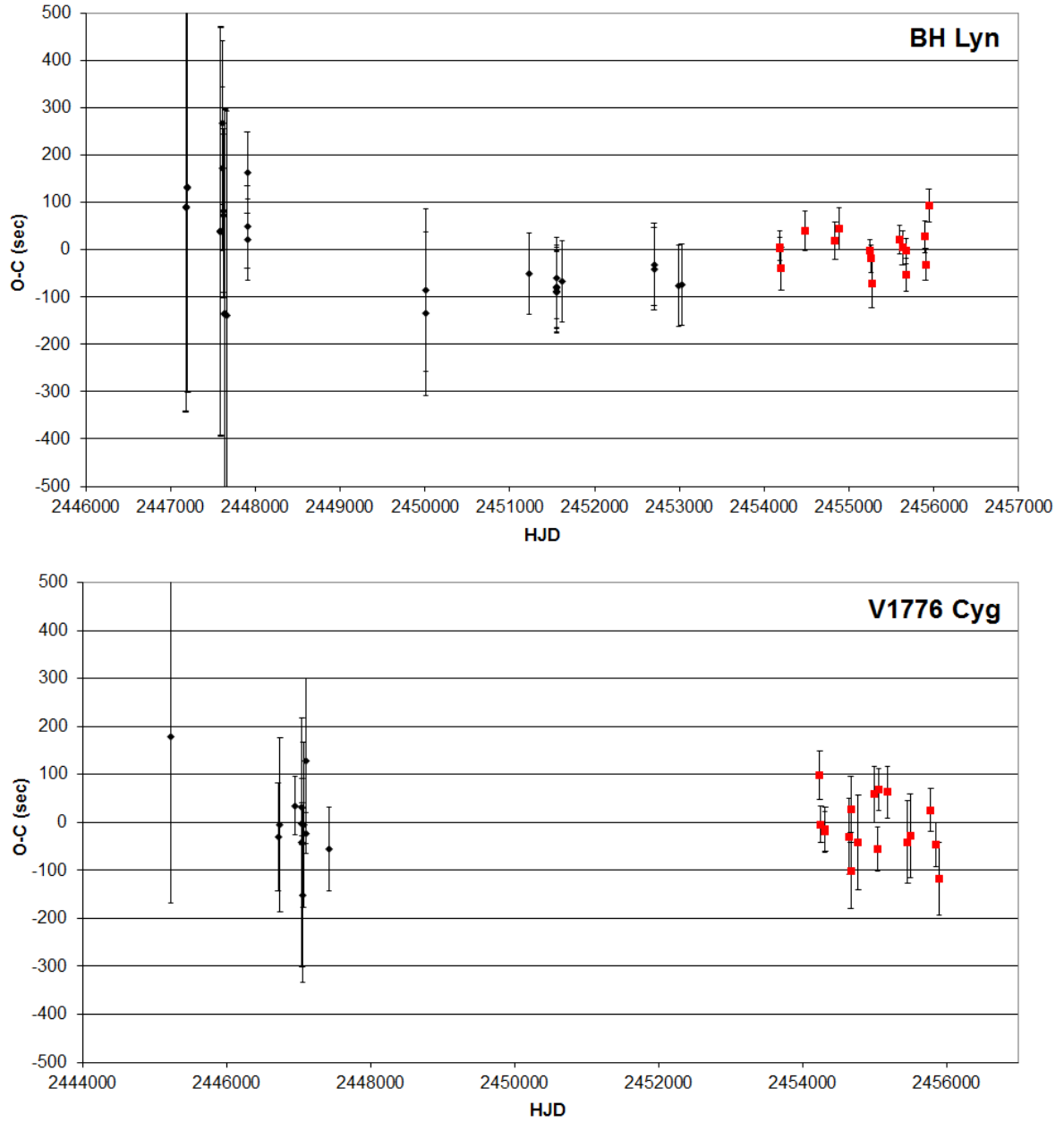


Figure 1. O–C diagrams with respect to the linear ephemerides in Table 3 for those SW Sex stars with $P_{orb} < 4$ hours which are consistent with constant orbital periods. Previously published observations are marked as black dots and new eclipse times as red squares in this and subsequent figures.

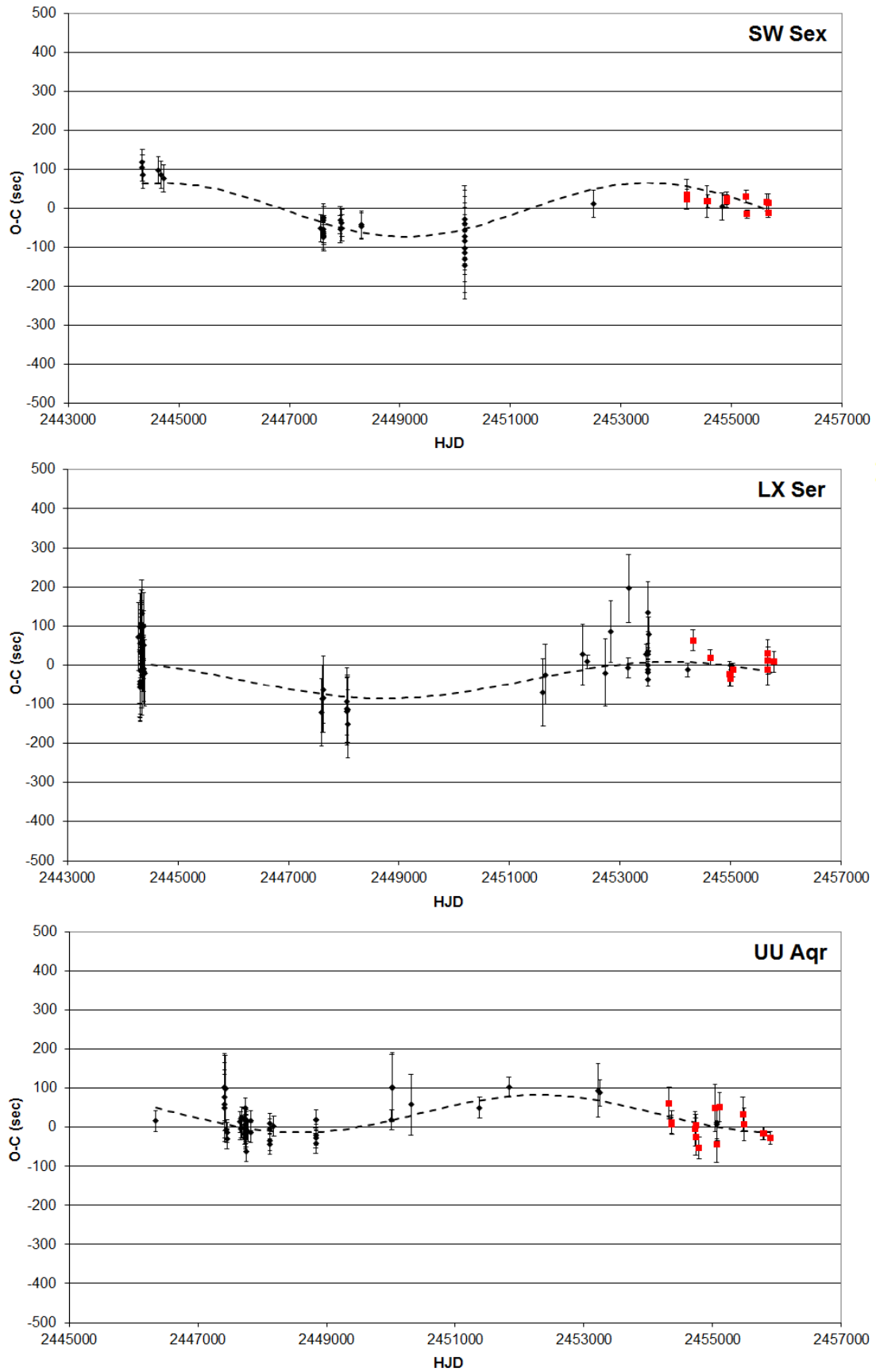


Figure 2. O–C diagrams with respect to the linear ephemerides in Table 3 for those SW Sex stars with $P_{orb} < 4$ hrs which show possible cyclical variation in orbital period (dashed lines).

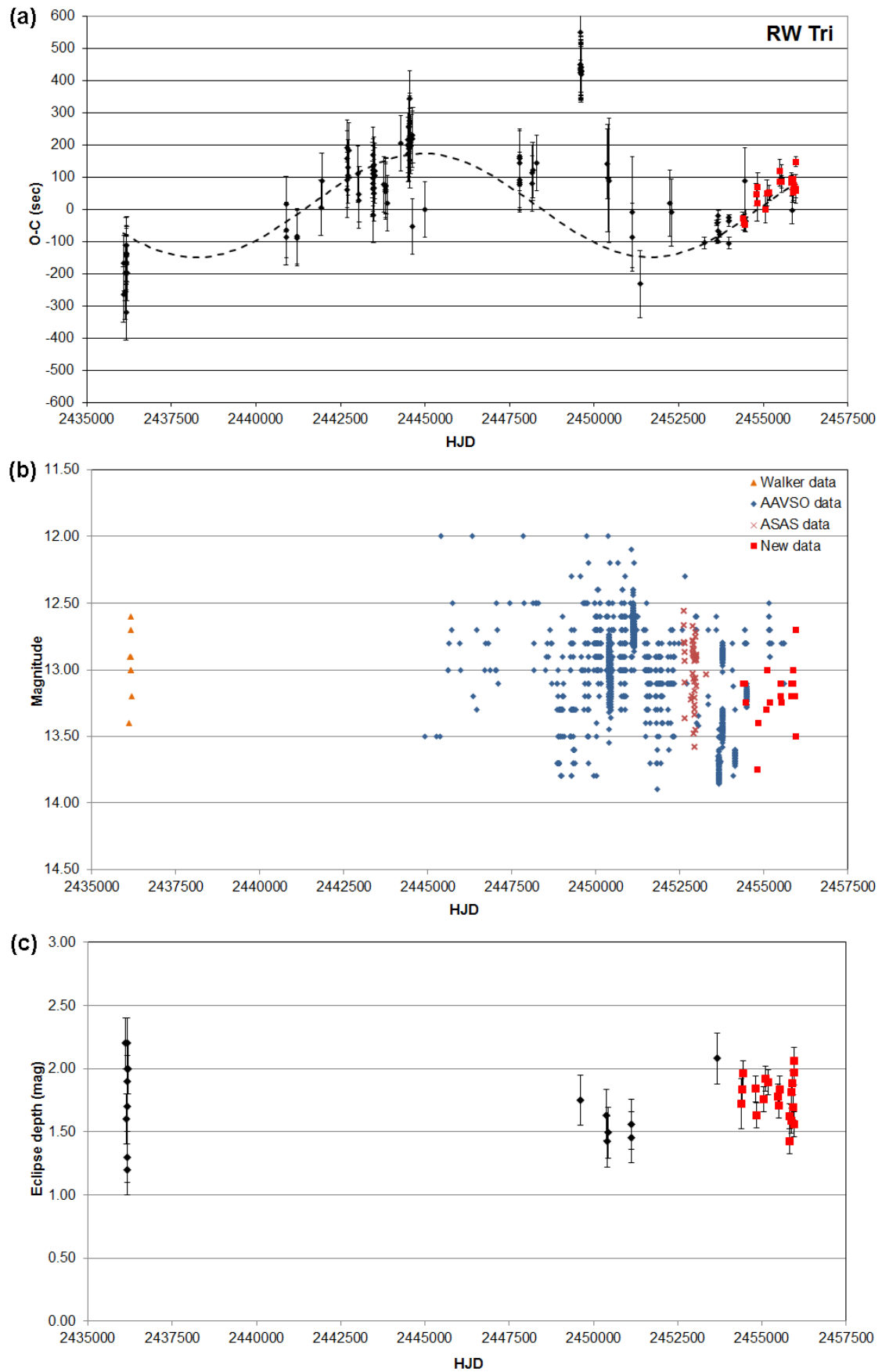


Figure 3. RW Tri: (a) O–C diagram with respect to a linear ephemeris showing a cyclical variation of orbital period (dashed line), (b) out-of-eclipse magnitude, and (c) eclipse depth.

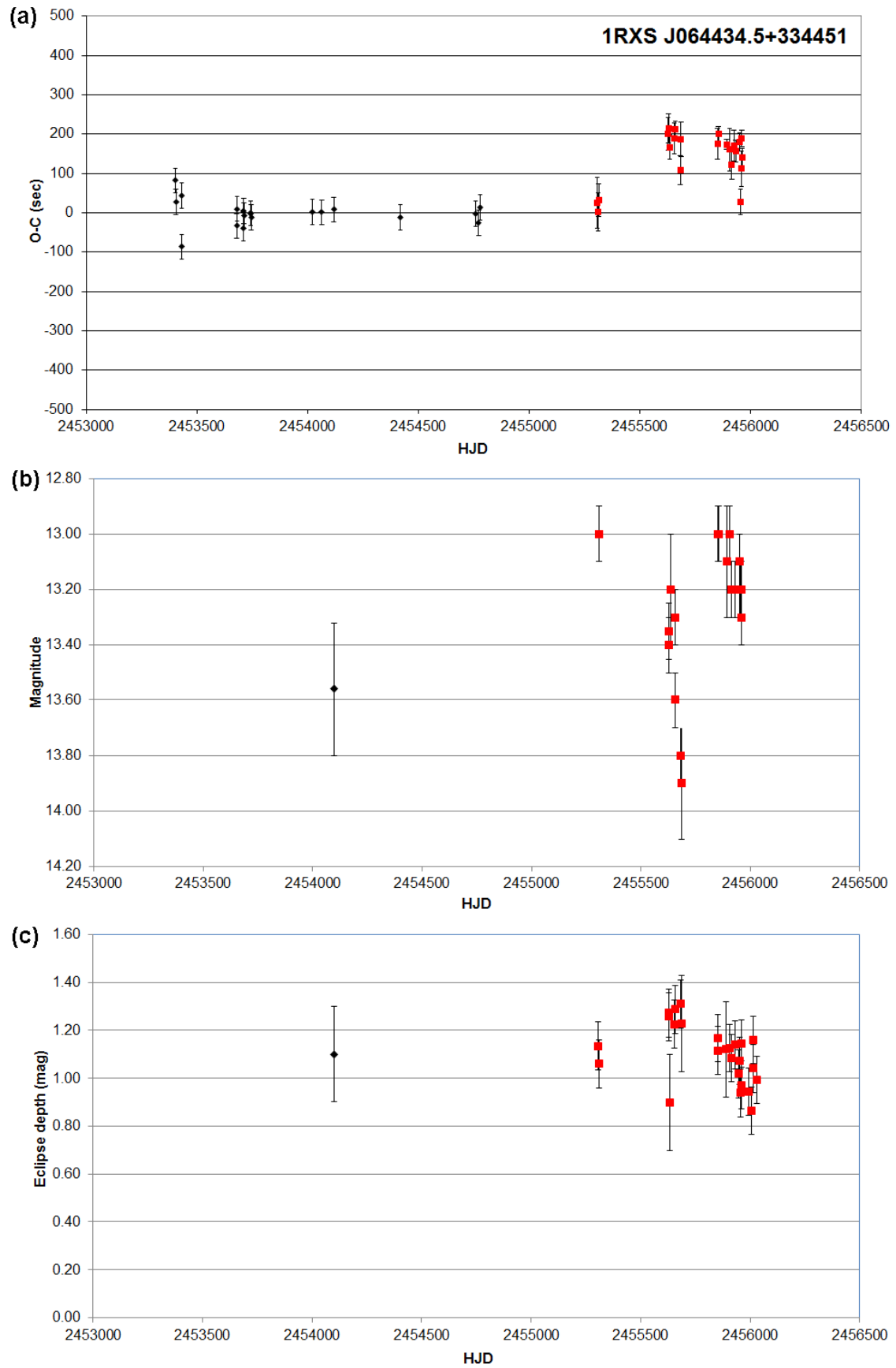


Figure 4. 1RXS J064434.5+334451: (a) O–C diagram with respect to a linear ephemeris for HJD < 2455500, (b) out-of-eclipse magnitude, and (c) eclipse depth.

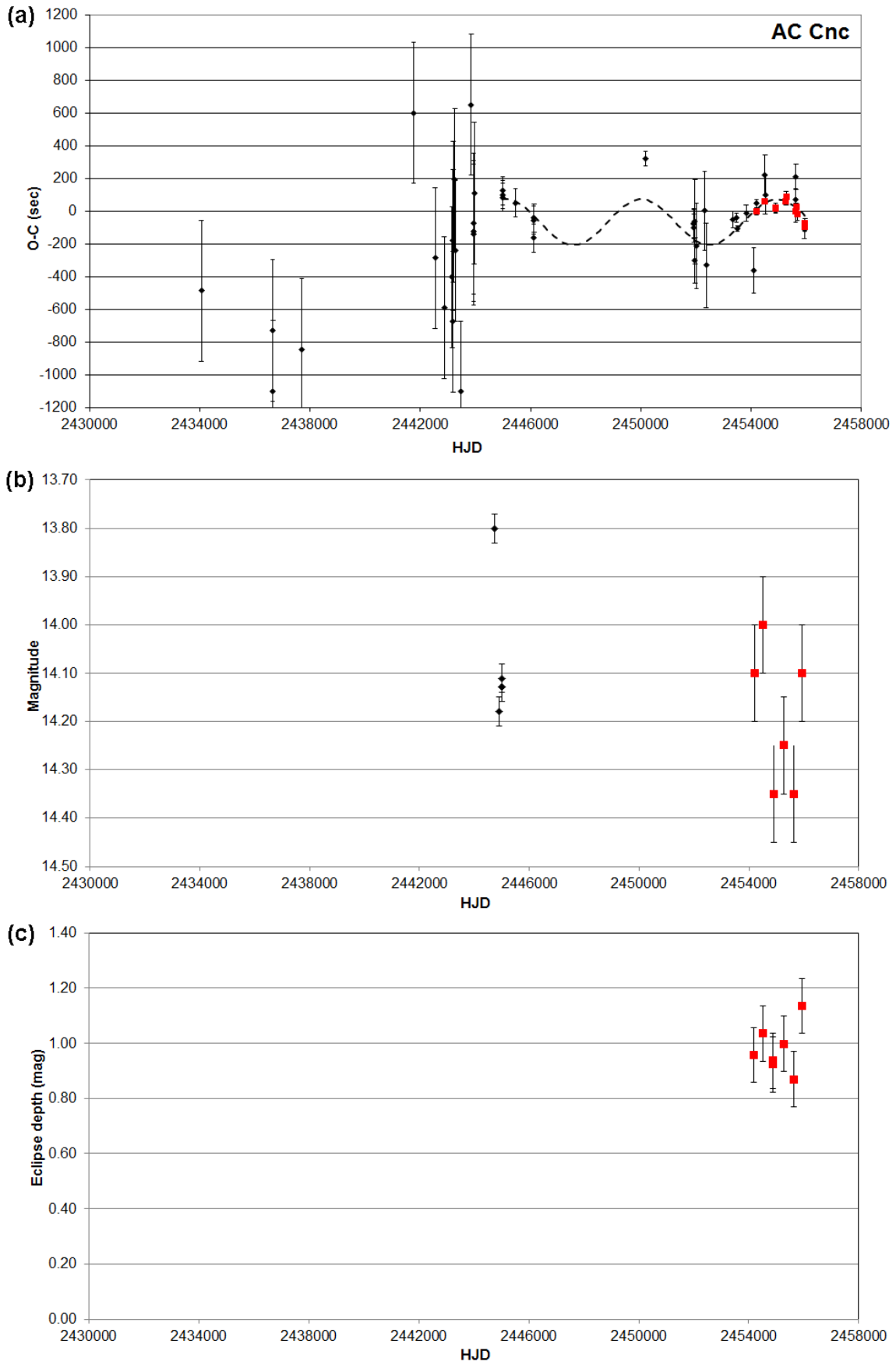


Figure 5. AC Cnc: (a) O–C diagram with respect to a linear ephemeris showing a cyclical variation of orbital period (dashed line), (b) out-of-eclipse magnitude, and (c) eclipse depth.

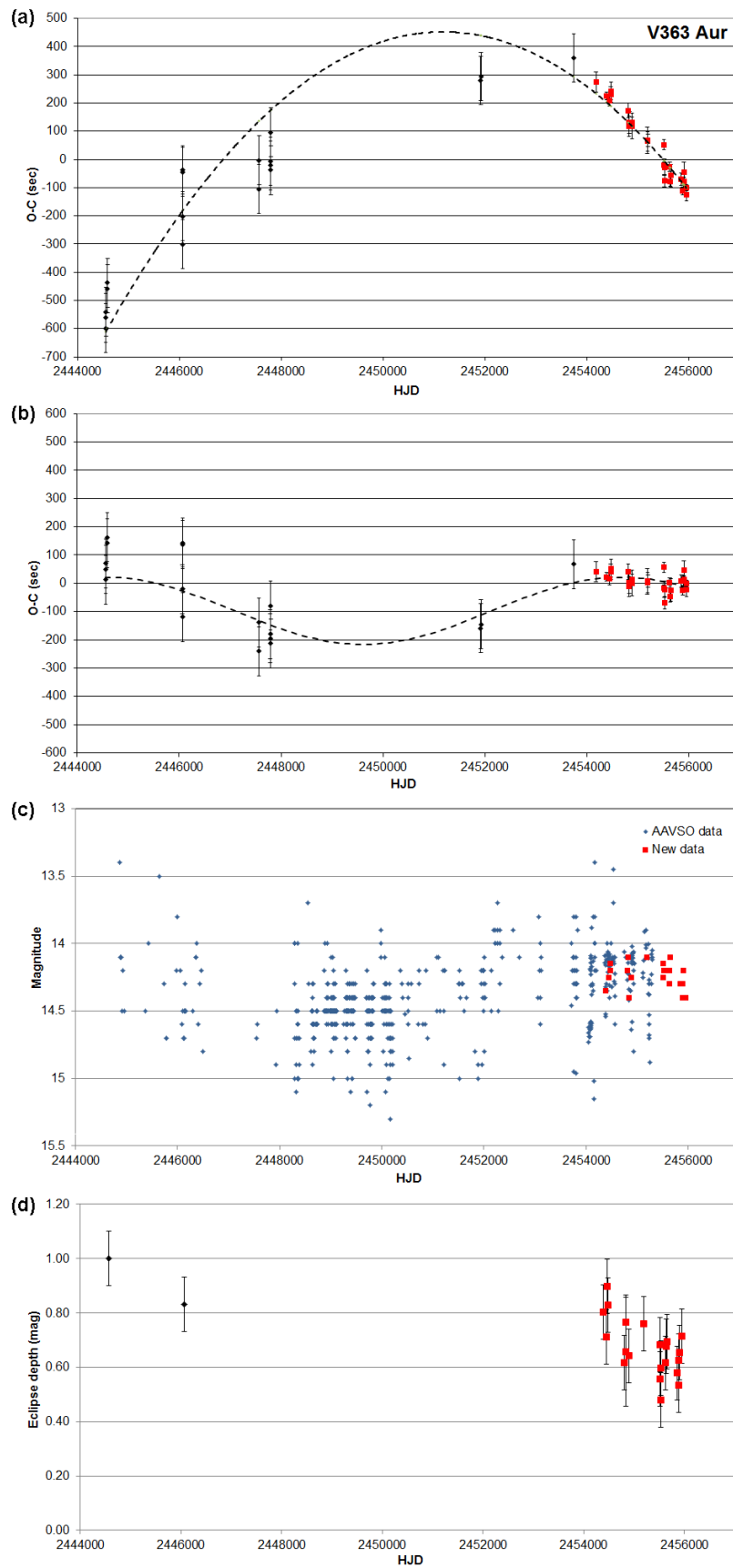


Figure 6. V363 Aur: (a) O–C diagram with respect to a linear ephemeris showing a quadratic ephemeris (dashed line), (b) O–C diagram with respect to a quadratic ephemeris showing a cyclical variation of orbital period (dashed line), (c) out-of-eclipse magnitude, and (d) eclipse depth.

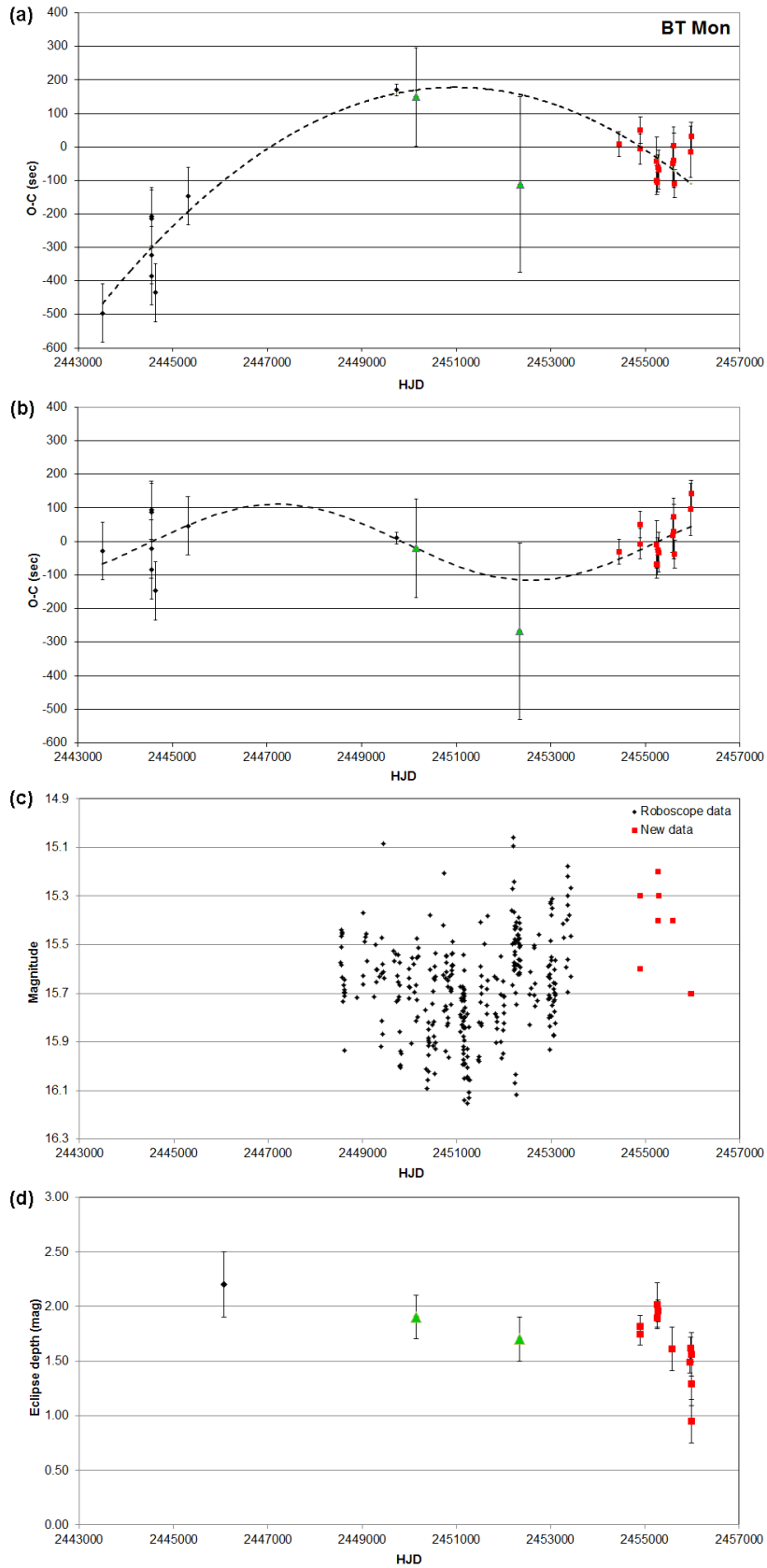


Figure 7. BT Mon: (a) O–C diagram with respect to a linear ephemeris showing a quadratic ephemeris (dashed line), (b) O–C diagram with respect to a quadratic ephemeris showing a cyclical variation of orbital period (dashed line), (c) out-of-eclipse magnitude, and (d) eclipse depth. Eclipses synthesised using Roboscope data are shown as green triangles.